Volume 335, number 2, 265–269 FEBS 13335 December 1993

Differential contribution by conserved glutamate residues to an ion-selectivity site in the L-type Ca^{2+} channel pore

Gabor Mikala**, Anthony Bahinski**, Atsuko Yatani, Shaoqing Tang, Arnold Schwartz*

Department of Pharmacology and Cell Biophysics, University of Cincinnati College of Medicine, Cincinnati, OH 45267-0575, USA

Received 17 September 1993; revised version received 18 October 1993

In voltage-gated cation channels, it is thought that residues responsible for ion-selectivity are located within the pore-lining SS1–SS2 segments. In this study, we compared the ion permeation properties of mutant calcium channels in which highly conserved glutamate residues, located at analogous positions in the SS2 regions of all four motifs, were individually replaced. All of the mutants exhibited a loss of selectivity for divalent over monovalent cations. However, the permeation properties of the individual mutants varied in a position dependent manner. The results provide strong evidence that these glutamate residues, positioned at equivalent locations in the aligned sequences, play significantly different roles in forming the selectivity barrier of the calcium channel, and are probably arranged in an asymmetrical manner inside the ion-conducting pore.

Calcium channel; Ion permeation; Site-directed mutagenesis; Pore structure; SS1–SS2 region

1. INTRODUCTION

Voltage-gated calcium channels form a unique class in the structurally homologous superfamily of voltage-gated ion channels, characterized by their high selectivity for calcium ions (Ca^{2+}) [1]. Recently, it has been shown that the highly conserved SS1–SS2 regions of the connecting loop between the S5 and S6 transmembrane helices of K^+ and Na^+ channels harbor critical residues that determine ion selectivity [2–4], conductance [5–7], as well as sensitivity to certain toxins [5,8–10] and transition metal ions [9,10]. It is postulated that these regions are able to fold to the membrane as a β-sheet to form a pore-lining surface [11]. In our previous study involving site-directed mutagenesis of the proposed ion-permeation pathway of an L-type cardiac Ca^{2+} channel [12], we determined that replacement of specific glutamate (Glu) residues of the SS2 regions with noncharged or oppositely charged residues resulted in a significant loss of selectivity of the channel for divalent over monovalent cations. In another study, it was shown that neutralization of the corresponding Glu residues in motifs III and IV of the brain BI-2 calcium channel caused a marked decrease in the Cd^{2+}-sensitivity of the channel [13]. These Glu residues are among the most conserved amino acids of the SS2 regions of Ca^{2+} channels. However, in Na^+ channels a lysine in motif III and an alanine in motif IV occupy the equivalent positions (Fig. 1). We suggest that these four highly conserved glutamates may form a Ca^{2+} binding site and may therefore contribute to ion selectivity and/or ion binding within the pore of Ca^{2+} channels.

In order to determine whether these highly conserved Glu residues, which occupy equivalent positions within the optimally aligned SS1–SS2 regions of the four motifs, contribute equally to the formation of an ion-selectivity site, we compared the permeation of Ba^{2+} and Na^+ ions through wild-type and mutant human cardiac Ca^{2+} channels. The glutamate residues in each of the four motifs were individually replaced by either an oppositely charged lysine, a noncharged glutamine or an alanine.

2. MATERIALS AND METHODS

2.1. *Construction of mutant calcium channels*

The construction of plasmids carrying cDNAs encoding the wild type (hHT-1) [14] and mutant calcium channels E334K, E1086K, E1086Q, and E1387A has been described previously [12]. The other mutants were synthesized using the polymerase chain reaction technique (PCR, Hoffman-LaRoche [21]). Mutants in motif I (E334Q), motif II (E677K, Q or A) and motif IV (E1387K or Q) were made within *Nco*I(246)/*Bam*HI(2498) or *Sse*8387I(3061)/*Eco*RI(3448) or *Bst*BI(4664)/*Sph*I(5598) cassettes, respectively. Oligonucleotides encoding the *Nco*I or *Eco*RI or *Sph*I recognition sites and carrying the desired single or double base mismatches served as mutagenesis primers, and oligonucleotides covering the *Bam*HI or *Sse*8387I or *Bst*BI sites served as primer-pairs. The PCR products were subcloned and sequenced to verify the presence of the desired mutations and the absence of unwanted random mutations. Verified cassettes were then ligated into hHT-1 to replace the corresponding *Nco*I/*Bam*HI, *Sse*8387I/*Eco*RI or *Bst*BI/*Sph*I segments. Double mutants were engineered as described in [12]. cRNAs specific for the wild type calcium channel α_1 subunit, mutant calcium channel α_1 subunits, skeletal muscle α_2 subunit [16] and heart β_a subunit [22] were synthesized as described previously [12].

*Corresponding author. Fax: (1) (513) 558 1778.

**These authors contributed equally and are considered co-first authors.

2.2. *Electrophysiology*

Oocytes were injected with a total of 40 nl of cRNA from wild-type human heart α_1-subunit or mutant α_1-subunit (0.1 $\mu g/\mu l$) together with skeletal muscle α_2 subunit (0.1 $\mu g/\mu l$) and heart β_a-subunit (0.1 $\mu g/\mu l$) and incubated in modified Barth's solution for 3–7 days prior to testing. Whole-cell currents were recorded with a two-microelectrode voltage-clamp [14]. Voltage and current electrodes (1–2 MΩ) were filled with 3 M KCl. The external solutions contained 40 mM $Ba(OH)_2$, 50 mM *N*-methyl-D-glucamine, 2 mM KOH, and 5 mM HEPES (pH 7.3 with methanesulfonic acid) for the Ba^{2+}-containing solution and 120 mM Na(OH), 1 mM $MgCl_2$, 2 mM KOH, 1 mM EGTA, and 5 mM HEPES (pH 7.3 with methanesulfonic acid) for the Na^+-containing solution. Current records were sampled at 2 ms intervals after low pass filtering at 0.2 kHz. Leakage and capacitative currents were subtracted using a P/4 protocol. In control experiments, voltage-activated Ba^{2+} currents were seen in ~30% of uninjected oocytes (less than 20 nA magnitude). We never observed inward currents in the Na^+-containing external solution in uninjected oocytes. In Na^+-containing external solution, current responses to potentials greater than +40 mV often showed biphasic or off-scale currents and are omitted from data points. All electrophysiological experiments were performed at room temperature (20–21°C). The data are presented as means ± S.E.

3. RESULTS

We compared the permeation of Ba^{2+} and Na^+ through wild-type and mutant Ca^{2+} channels. Fig. 2 shows families of whole-cell currents recorded from *Xenopus* oocytes injected with cRNA specific for the wild-type human cardiac Ca^{2+} channel (Fig. 2A), the mutant E334K (Fig. 2B), E677K (Fig. 2C) and E1387K (Fig. 2D). All oocytes were coinjected with skeletal α_2- and cardiac βa-subunit specific cRNAs in order to maximize current density.

Expression of the wild-type cardiac Ca^{2+} channel, resulted in large inward voltage-dependent currents with 40 mM Ba^{2+} as the charge carrier. These currents reached a peak value around +20 mV and reversed at potentials greater than +60 mV (Table I). Replacement of external Ba^{2+} with Na^+ resulted in a marked decrease in inward currents and the appearance of outward currents at positive potentials. The Ba^{2+}-free external solution contained 1 mM Mg^{2+} in order to prevent destabilization of the oocyte membrane, which rapidly occurred in the total absence of external divalent cations.

The mutants E334K and E1086K were ineffective in permeating Ba^{2+} ions. These mutants exhibited small inward currents in the presence of external Ba^{2+} which reached a peak around 0 mV and then quickly reversed to become outward at more positive test potentials. The peak inward current amplitude in Ba^{2+}-containing external solution was 10–20 nA, comparable to the magnitude of endogenous oocyte Ca^{2+} channel currents. Re-

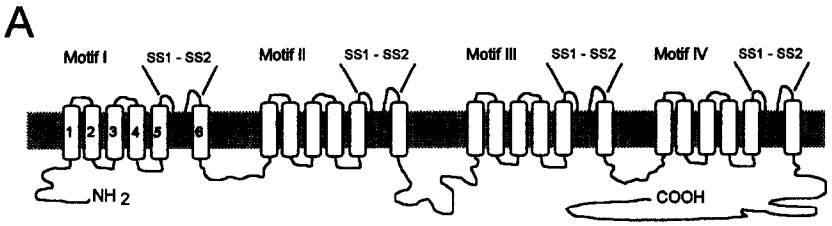

B

Motif I			Motif III		
C	FAFAMLTVFQCITMEGWTD	(320 - 338)	C	VLAAMMALFTVSTFEGWPE	(1072 - 1090)
D	FAFAMLTVFQCITMEGWTD	(350 - 368)	D	VLSAMMALFTVSTFEGWPA	(1087 - 1105)
Sk	FGFSMLTVYQCITMEGWTD	(278 - 296)	Sk	VLSAMMSLFTVSTFEGWPQ	(1000 - 1018)
BI	ILFAVLTVFQCITMEGWTD	(304 - 322)	BI	VLWALLTLFTVSTGEGWPQ	(1455 - 1473)
BII	ILFAVLTVFQCITMEGWTT	(295 - 313)	BII	IIWALLTLFTVSTGEGWPQ	(1348 - 1363)
BIII	ILFAILTVFQCITMEGWTD	(300 - 318)	BIII	VLWALLTLFTVSTGEGWPM	(1356 - 1374)
Na	FAWAFLALFRLMTQDCWER	(359 - 377)	Na	VGAGYLALLQVATFKGWMD	(1407 - 1425)

Motif II			Motif IV		
C	QSLLTVFQILTGEDWNS	(665 - 681)	C	QAVLLLFRCATGEAWQD	(1375 - 1391)
D	QALLTVFQILTGEDWNA	(693 - 709)	D	QAVLLLFRCATGEAWQE	(1394 - 1410)
Sk	QALISVFQVLTGEDWNS	(602 - 618)	Sk	QAVLLLFRCATGEAWQE	(1311 - 1327)
BI	AAIMTVFQILTGEDWNE	(656 - 672)	BI	QALMLLFRSATGEAWHN	(1753 - 1769)
BII	AAIMTVFQILTGEDWNE	(645 - 661)	BII	GSLMLLFRSATGEAWQE	(1641 - 1657)
BIII	AAILTVFQILTGEDWNA	(652 - 668)	BIII	QALMLLFRSATGEAWHE	(1646 - 1662)
Na	HAFLIIFRILCGE-WIE	(889 - 904)	Na	NSMLCLFQITTSAGWDG	(1701 - 1717)

Fig. 1. Comparison of the SS1–SS2 regions of all six types of cloned Ca^{2+}-channels and a representative Na^+-channel. (A) The four motifs of the Ca^{2+} channel are displayed linearly with six putative transmembrane α-helices (S1–S6) represented by cylinders, in each of the four motifs. The SS1–SS2 region between putative transmembrane segments S5 and S6 has been placed in the membrane. (B) Amino acids (in single-letter code) of the proposed SS1–SS2 regions, optimally aligned to the human cardiac Ca^{2+} channel sequence C; ref. [14]. The other channel sequences displayed are: D, human neuroendocrine L-type Ca^{2+} channel [15]; Sk, rabbit skeletal muscle L-type Ca^{2+} channel [16]; BI, rabbit brain BI-2 calcium channel [17]; BII, rabbit brain BII-2 calcium channel [18]; BIII, rabbit brain BIII (N-type) Ca^{2+} channel [19]; Na, rat heart (HI) sodium channel [20]. The numbers of the amino acid residues are indicated on the right-hand side of each sequence. The glutamate residues investigated are shown in boldface.

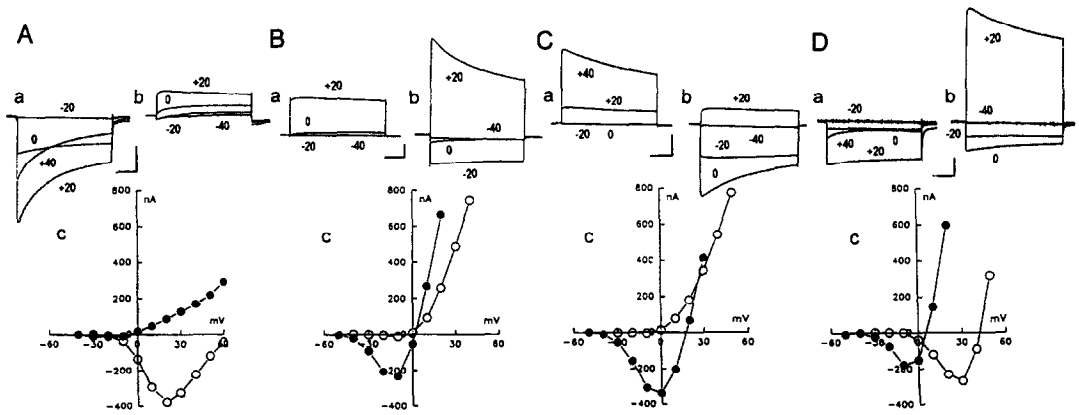

Fig. 2. Mutation of glutamate residues in the putative pore region in each of the four motifs of the Ca^{2+} channel display different ion-selectivities. Whole-cell currents were recorded from oocytes injected with cRNAs encoding wild-type (A), and mutant channels E334K (B), E677K (C), and E1387K (D) in Ba^{2+}-(a) or Na^{+}-(b) containing external solution. The representative whole-cell currents are shown above and the current–voltage relationships are shown below. Data recorded in Ba^{2+}-containing external solution are shown using open symbols, whereas those obtained in Na^{+}-containing external solution are shown with filled symbols.

placement of external Ba^{2+} with Na^{+} resulted in a dramatic increase in inward current.

Expression of mutant E677K also produced small Ba^{2+} currents with slightly different properties as compared to those obtained from mutants in motifs I or III. The small inward Ba^{2+} current peaked at +8 mV and the reversal potential was +12 mV. Mutant E677K exhibited the largest ratio of peak Na^{+} versus peak Ba^{2+} currents (~ 30:1). In addition, the peak of the current–voltage relationship and the reversal potential were both shifted to more positive potentials, compared to those for the mutants E334K and E1086K.

Expression of the Ca^{2+} channel mutant E1387K produced channels with unique properties. With 40 mM Ba^{2+} as the charge carrier, large inward currents (greater than 200 nA) were detected with a peak amplitude around +20 mV. The reversal potential (+32.4 ± 1.1 mV) was shifted to more negative potentials (compared to the wild-type), indicating an increased efflux of K^{+} ions through the channel at more positive potentials. Interestingly, changing to a Na^{+}-containing external solution caused only a shift in the *I–V* curve to more negative potentials but did not significantly change the peak current amplitude. The reversal potential measured in the Na^{+}-containing solution was not significantly different from that measured for the analogous mutants in motif I or III.

To gain further insight into the role of these glutamate residues and to confirm the unique differences obtained by substituting with lysine, we investigated the effect of more conservative changes. When the glutamates were neutralized by replacement with a non-charged glutamine, mutant E1086Q (in motif III) exhibited the greatest monovalent permeation. In addition, E1086Q exhibited the largest leftward shift in the reversal potential in its class measured with Ba^{2+} as the charge carrier. When the glutamate residue in motifs II, III and IV were replaced by alanine, the channel mutant E1387A (in motif IV) stood out as the mutant exhibiting the smallest difference of all the mutants in permeation properties, compared to the wild-type.

Double mutants, involving motif III and IV, showed a further increase in monovalent permeation compared to the properties of either of the individual single mutants. Quite interestingly, when the glutamates were neutralized in both motifs (III and IV), a significant Ba^{2+} permeability was retained (Table I).

4. DISCUSSION

In the present study, we show that individually substituting glutamate residues with lysine, glutamine or alanine in the SS2 segments of each of the four motifs of the human cardiac L-type Ca^{2+} channel differentially alters the ion-permeation properties of the channel. This is in agreement with a previous study [13], in which Gln residues were substituted for Glu at the corresponding positions of the brain BI-2 calcium channel, in motifs III and IV, and it was shown that these residues were not functionally identical.

Substitution of the negatively charged glutamates in motifs I, II and III with positively charged lysine had deleterious effects on divalent cation permeation. However, Na^{+} readily passed through the channels in a voltage-dependent manner suggesting that there were no gross structural changes in the channel structure. The lack of any significant Ba^{2+} permeation through mutants E334K, E667K and E1086K indicates that these three glutamate residues may be intimately involved in the formation of high affinity divalent binding sites within the Ca^{2+} channel pore [23].

Substitution of Glu^{677} with Lys in motif II exhibited similar but not identical properties to the replacement of the corresponding residues in motifs I and III. This

residue is unique in its position in the SS2 regions since in the primary structure its neighbor is a negatively charged aspartate. Therefore, the change in the local charge-distribution caused by the introduction of the lysine residue might be smaller than in the case of motif I or III mutants. Nevertheless, it is also possible that the higher apparent Na^+ permeation is caused by a decrease in the level of Mg^{2+} block [24] or a relative decrease in outward K^+ permeation.

Clearly, a mutant with unique properties was obtained by substitution of lysine for Glu^{1387}, in motif IV. The extra positive charge introduced into the putative pore resulted in an increase in monovalent permeation without abolishing the divalent permeability. It is likely that this residue (Glu^{1387}) is positioned differently from the others investigated: possibly located near the extracellular mouth or within a vestibule which opens into a narrow region of the pore.

The effects of more conservative substitutions for the investigated glutamates provided further support to our finding of motif-to-motif differences. In these experiments, motif III (Glu^{1086}) was found to be most sensitive to replacement with glutamine. Motif IV (Glu^{1387}) was the least sensitive to substitution by either glutamine or alanine. These data are consistent with an asymmetrical arrangement of groups having outer sphere interactions with the permeant divalent cations rather than with a planar configuration of these residues. A similar conclusion (for motifs III and IV) was drawn for the brain BI Ca^{2+} channel, in which neutralization of Glu^{1469} (in motif III) caused a 200-fold decrease in Cd^{2+} sensitivity of the channel [13]. However, neutralization of the analogous residue in the L-type Ca^{2+} channel resulted in only a 15-fold decrease in Cd^{2+} sensitivity (IC_{50}'s for wild type and E1086Q were 0.9 mM and 13.3 mM, respectively). Nevertheless, a similar shift was observed in the reversal potential (Table I). These data illustrate possible differences in the ion permeation pathway between these two different Ca^{2+} channel types.

In two recent abstracts [25,26], each of the four glutamate residues in the pore-lining region was also found to contribute unequally to divalent cation binding. In the same reports, it is suggested that no other high affinity binding site exists independently of the four glutamates. Our results showing Ba^{2+} permeation through specific double mutant channels in which two of the four glutamate residues were neutralized, indicate that other residues (or groups of the peptide backbone) in addition to the four glutamate residues may contribute to divalent cation binding within the pore.

It is tempting to compare the Na^+ and Ca^{2+} channel ion selectivity structures. In Na^+ channels, K^{1422} and A^{1714} and to a smaller extent E^{387} were found to be critical for determining the ion selectivity of the channel [3]. Since the SS2 sequences are quite different among the individual motifs, these findings represented the asymmetry of the sodium channel pore structure. In Ca^{2+} channels, where a largely symmetrical pore structure may be predicted based on the sequence homology in the SS2 regions, the pore model seems to develop into

Table I

Properties of wild-type and mutant Ca^{2+} channels

Motif		In 120 mM Na^+				In 40 mM Ba^{2+}				Ratio	
		Amplitude (nA)	Peak I–V (mV)	App E_{rev} (mV)	n	Amplitude (nA)	Peak I–V (mV)	App E_{rev} (mV)	n	peak I_{Na^+}/ peak $I_{Ba^{2+}}$	n
	hHT*	37.1 ± 21.1	−13.4 ± 2.3	+ 2.7 ± 2.3	6	447.0 ± 136.0	+21.8 ± 1.1	+67.3 ± 3.5	6	0.06 ± 0.01	5
I	E334K*	140.8 ± 28.1	−12.0 ± 1.3	+ 1.1 ± 1.1	8	16.7 ± 6.5	− 0.1 ± 4.8	+ 3.4 ± 5.3	5	14.10 ± 3.60	5
II	E677K	388.2 ± 56.8	− 4.6 ± 1.2	+15.3 ± 1.3	11	33.1 ± 10.3	+ 7.9 ± 2.5	+12.3 ± 3.2	10	28.80 ± 7.50	10
III	E1086K*	62.5 ± 13.1	−10.8 ± 1.0	+ 0.6 ± 0.7	6	11.9 ± 2.4	− 2.8 ± 1.7	+ 4.2 ± 1.0	6	8.25 ± 2.40	6
IV	E1387K	219.9 ± 78.3	− 9.1 ± 1.7	+ 1.9 ± 1.8	8	231.6 ± 29.2	+19.5 ± 1.4	+32.4 ± 1.1	17	0.84 ± 0.07	7
I	E334Q	76.3 ± 26.9	− 8.5 ± 1.4	+ 2.3 ± 1.6	8	165.7 ± 15.8	+17.8 ± 1.0	+43.3 ± 1.1	12	0.50 ± 0.10	8
II	E677Q	98.9 ± 19.6	−14.2 ± 2.2	+ 0.3 ± 2.3	13	345.9 ± 22.7	+17.7 ± 0.6	+42.3 ± 0.9	15	0.27 ± 0.04	13
III	E1086Q*	164.1 ± 11.4	− 8.2 ± 0.4	+ 2.2 ± 0.3	4	175.3 ± 25.0	+15.9 ± 0.4	+36.9 ± 0.6	7	1.15 ± 0.11	8
IV	E1387Q	55.0 ± 9.2	−20.2 ± 2.2	−11.0 ± 2.7	9	477.4 ± 50.1	+21.5 ± 1.0	+41.6 ± 2.0	10	0.12 ± 0.01	9
II	E677A	200.7 ± 69.2	− 9.5 ± 2.1	+ 2.6 ± 1.8	7	373.0 ± 90.6	+22.1 ± 1.7	+43.4 ± 1.8	11	0.33 ± 0.10	5
III	E1086A	305.4 ± 133.3	−15.4 ± 1.9	− 5.0 ± 3.2	7	667.6 ± 148.5	+16.2 ± 1.6	+47.0 ± 4.3	11	0.33 ± 0.18	4
IV	E1387A*	60.3 ± 11.4	−13.3 ± 1.2	− 4.0 ± 1.1	9	579.6 ± 76.3	+27.1 ± 0.8	+61.0 ± 1.5	11	0.10 ± 0.01	22
III, IV	E1086K, E1387A*	243.2 ± 63.4	−11.8 ± 2.0	+ 4.1 ± 0.8	6	18.1 ± 2.1	− 2.3 ± 1.4	+ 3.1 ± 1.7	8	14.80 ± 2.25	11
III, IV	E1086Q, E1387A	453.2 ± 195.3	−18.4 ± 2.6	− 5.1 ± 2.3	7	110.2 ± 29.3	+ 1.8 ± 1.1	+13.0 ± 1.0	9	3.60 ± 1.20	5
III, IV	E1086A, E1387A	29.9 ± 6.4	−15.8 ± 2.6	− 6.5 ± 3.8	4	121.6 ± 37.2	+14.1 ± 1.6	+24.4 ± 1.6	7	0.57 ± 0.04	4

Data are given as mean ± S.E.M. (n = number of experiments). The holding potential was between −80 and −60 mV and the relative ratio was calculated by dividing peak inward currents in the Na^+ solution by those obtained in the Ba^{2+} solution. Apparent reversal potential ($AppE_{rev}$) was extrapolated from the I–V relationships. *Values from [12].

an unexpectedly complex and asymmetrical one. In fact, our data are consistent with the idea that these glutamate residues form an array of ligand groups within the channel pore which interact with the permeating ion and not a fixed or discrete high affinity binding site [23].

Acknowledgements: This research was supported in part by National Institutes of Health Grants PO1 HL22619–15, 5R37 HL43231–04 and T32 HL07386–16 (to A.S.), by the American Heart Association Grant 93012860 (to A.Y.) and by the Tanabe Seiyaku Fund for Molecular Biophysics and Physiology. Drs. Bahinski and Mikala are Postdoctoral Fellows of the Program of Excellence in the Molecular Biology of Heart and Lung (National Institutes of Health Grant HL 41496–04). The authors would like to thank Dr. Gyula Varadi for critical reviewing of the manuscript and Chanda Ramdhian for expert technical assistance with *Xenopus* oocytes.

REFERENCES

[1] Tsien, R.W., Hess, P., McCleskey, E.W. and Rosenberg, R.L. (1987) Annu. Rev. Biophys. Chem. 16, 265–290.
[2] Yool, A.F. and Schwarz, T.L. (1991) Nature 349, 700–704.
[3] Heinemann, S.H., Terlau, H., Stühmer, W., Imoto, K. and Numa, S. (1992) Nature 356, 441–443.
[4] Mackinnon, R. and Yellen, G. (1990) Science 250, 276–279.
[5] Terlau, H., Heinemann, S.H., Stühmer, W., Pusch, M., Conti, F., Imoto, K. and Numa, S. (1991) FEBS Lett. 293, 93–96.
[6] Hartmann, H.A., Kirsch, G.E., Drewe, J.A., Taglialatela, M., Joho, R.H. and Brown, T.A. (1991) Science 251, 942–944.
[7] Heginbotham, L., Thromson, T. and MacKinnon, R. (1992) Science 258, 1152–1155.
[8] Kontis, K.T. and Goldin, A.L. (1993) Mol. Pharmacol. 43, 635–644.
[9] Backx, P.H., Yue, D.T., Lawrence, J.H., Marban, E. and Tomaselli, G.F. (1992) Science 257, 248–251.
[10] Satin, J., Kyle, J.W., Chen, M., Bell, P., Cribbs, L.L., Fozzard, H.A. and Rogart, R.B. (1992) Science 256, 1202–1205.
[11] Guy, H.R. and Conti, F. (1990) Trends. Neurosci 13, 201–206.
[12] Tang, S., Mikala, G., Bahinski, A., Yatani, A., Varadi, G. and Schwartz, A. (1993) J. Biol. Chem. 268, 13026–13029.
[13] Kim, M., Mori, T., Sun, L., Imoto, K. and Mori, Y. (1993) FEBS Lett. 318, 145–148.
[14] Schultz, D., Mikala, G., Yatani, A., Engle, D.B., Iles, D.E., Segers, B., Sinke, R.J., Weghuis, D., Klöckner, U., Wakamori, M., Wang, J., Melvin, D., Varadi, G. and Schwartz, A. (1993) Proc. Natl. Acad. Sci. USA 90, 6228–6232.
[15] Williams, M.E., Feldman, D.H., McCue, A.F., Brenner, R., Velecebi, G., Ellis, S.B. and Harpold, M.M. (1992) Neuron 8, 71–84.
[16] Ellis, S.B., Williams, M.E., Ways, N.R., Brenner, R., Sharp, A.H., Hewing, A.T., Campbell, K.P., McKenna, E., Koch, W.J., Hui, A., Schwartz, A. and Harpold, M.M. (1988) Science 241, 1661–1664.
[17] Mori, Y., Friedrich, T., Kim, M., Mikami, A., Nakai, J., Ruth, P., Bosse, E., Hofman, F., Flockerzi, V., Furuichi, T., Mikoshiba, K., Imoto, K., Tanabe, T. and Numa, S. (1991) Nature 350, 398–402.
[18] Niidome, T., Kim, M., Friedrich, T. and Mori, Y. (1992) FEBS Lett. 308, 7–13.
[19] Fujita, Y., Myulieff, M., Dirksen, R.T., Kim, M., Niidome, T., Nakai, J., Friedrich, T., Tanabe, N., Miyata, T., Furuichi, T., Fusumata, D., Mikoshiba, K., Mori, Y. and Beam, K.G. (1993) Neuron 10, 85–598.
[20] Rogart, R.B., Cribbs, L.L., Muglia, L.K., Kephant, D.D. and Kaiser, M.W. (1989) Proc. Natl. Acad. Sci. USA 86, 8170–8174.
[21] Erlich, H.A. (1989) PCR Technology, Stockton Press, New York.
[22] Collin, T., Wang, J., Nargeot, J. and Schwartz, A. (1993) Circulation Res. 72, 1337–1344.
[23] Kuo, C-C. and Hess, P. (1993) J. Physiol. 466, 657–682.
[24] Matsuda, H. (1986) Pflügers Arch. 407, 465–475.
[25] Sather, W.A., Ellinor, P.T., Yang, J., Zhang, J.-F., Wang, H.Y.-C. and Tsien, R. (1993) Soc. Neurosci. Abstr. 19, 11.1.
[26] Yang, J., Ellinor, P.T., Sather, W.A., Zhang, J.-F., Wang, H.Y.-C. and Tsien, R.W. (1993) Soc. Neurosci. Abstr. 19, 11.2.